

ULTRA-HIGH RESOLUTION MR ELASTOGRAPHY OF THE HUMAN BRAIN: TECHNICAL DEVELOPMENT AND APPLICATIONS IN AGING AND ALZHEIMER'S DISEASE

E. Triolo (1), O. Khegai (2), T. Hedden (3), P. Balchandani (2), M. Kurt (1,2)

(1) Department of Mechanical Engineering, University of Washington, Seattle, WA, USA

(2) The Biomedical Engineering and Imaging Institute, Icahn School of Medicine at Mount Sinai, New York City, NY, USA

(3) Graduate School of Biomedical Sciences, Icahn School of Medicine at Mount Sinai, New York City, NY, USA

INTRODUCTION

Magnetic resonance elastography (MRE) is a technique for determining the mechanical response of tissues using applied harmonic deformation and motion-sensitive MRI¹. Performing MRE on brain tissue can provide information on different structures within brain tissue based on their mechanical properties, which can then be used to diagnose pathologies such as Alzheimer's disease (AD) and dementias, or indicate disease progression²⁻⁶. Studies using MRE to investigate the mechanical properties of the human brain are most commonly performed at conventional field strength (3 Tesla (T) or 1.5T), although there have been a few attempts at the ultra-high field strength, 7T^{7,8}, in an attempt to achieve higher resolution scans. Aiming for higher resolution scans of the human brain at 7T, MRE presents unique challenges of decreased octahedral shear strain-based signal-to-noise ratio (OSS-SNR)⁹ and lower shear wave motion sensitivity. Additionally, it has been shown that quantitative values of MRE, i.e., the magnitude of the complex shear modulus estimate ($|G^*|$), are sensitive to changes in OSS-SNR¹⁰, so 7T MRE can present a challenge of not only quality, but accuracy.

Performing MRE at 7T, and more specifically at high resolution, proves to be an attractive option for investigations into small brain structures, such as in the progression in Alzheimer's disease. Early diagnosis of Alzheimer's disease is still challenging, because of the subtlety of the microstructural changes it initially causes in the brain and the difficulty of identifying them with traditional neuroimaging techniques such as MRI, PET, or CT scans. Recent evidence has revealed that the neurodegeneration characterizing AD is accompanied by effective tissue softening, which can be quantified *in vivo* using MRE²⁻⁶. However, MRE at conventional field strengths has a resolution limitation in studying finer microstructure details, such as hippocampal subfields, that are important in the investigation of AD tissue microstructure. *Overall, this work seeks to investigate advanced reconstruction and noise reduction techniques to improve accuracy of*

ultra-high field (7T) MRE in determining the mechanical properties of small brain tissue structures, with applications in aging and early detection of dementias.

METHODS

Full brain coverage MRE using our custom 2D multi-slice SE-EPI 7T MRE sequence^{11,12} was performed on twenty healthy human subjects (young adults, Avg. Age 26.9 ± 3.4 years) at 1.1mm^3 at 50Hz vibration frequency, using a 32-channel head coil (Nova Medical) on a 7T Siemens Magnetom MRI Scanner. Using the same methods, MRE was also performed on a custom silicone MRE phantom (CIRS 049)¹¹ with 20mm diameter spherical inclusions. The custom MRE sequence was synchronized with our custom pneumatic acoustic actuator^{11,13} by TTL triggering at the beginning of every TR (TR/slice=140ms, TE=65ms, GRAPPA=3, Partial Fourier=7/8). We also performed 7T MRE on our phantom at a resolution of 2.5mm^3 for comparison (GRAPPA=2).

For the scanner-reconstructed image series, we employed the MP-PCA denoising¹⁴ and our Algebraic Inversion of the Helmholtz Equation (AIDE) to calculate $|G^*|$ ¹². To improve the default scanner reconstruction method, we used Gadgetron¹⁵, an open-source MRI image reconstruction software, on the raw data files to generate magnitude and phase images before performing the same pre-processing and inversion method. We also calculated OSS-SNR⁹ after each post-processing method after performing SEGUE¹⁶ unwrapping on

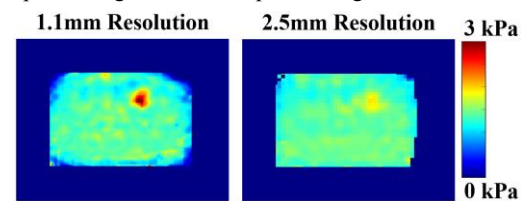


Figure 1: Custom Phantom with Spherical Inclusions Scanned at 7T Using Low and High Resolutions

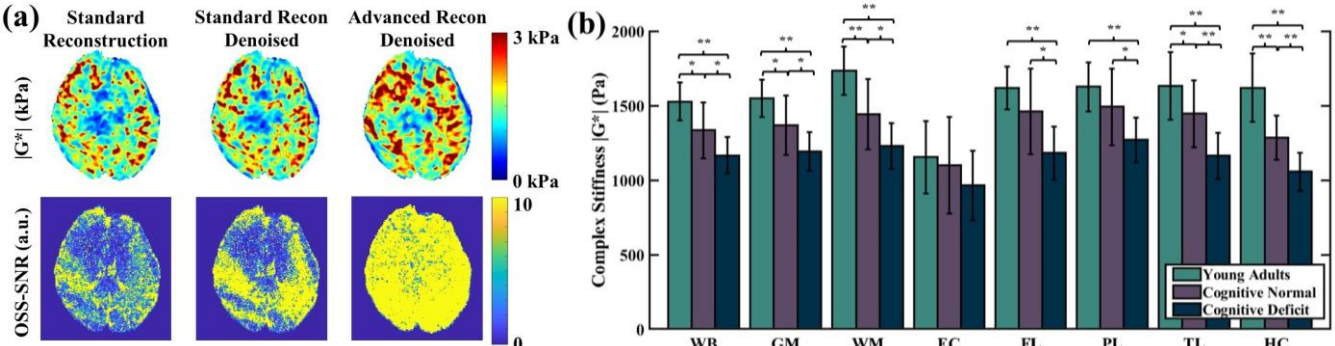


Figure 2: (a) High resolution Elastograms and OSS-SNRs with Advanced Reconstruction methods in One Young, Healthy Subject. (b) Average $|G^*|$ for Young Adults, CN, and CD individuals in all Segmented Brain Regions (* $p<0.05$, ** $p<0.01$)

the displacement fields. Segmentation of whole brain (WB), all gray matter (GM), all white matter (WM), the Entorhinal Cortex (EC), Frontal Lobe (FL), Parietal Lobe (PL), Temporal Lobe (TL), and Hippocampus (HC) were performed on the T1 (0.7mm^3) scans using Freesurfer¹⁷ and were co-registered SPM¹⁸. Differences between WB post-processing groups were analyzed using a one-way, repeated measures ANOVA with multiple comparisons.

Using the previously described 1.1mm^3 7T acquisition, denoising¹³, advanced reconstruction, and segmentation, full brain coverage 7T MRE was performed on six human subjects that presented with cognitive deficits (CD, Avg. age 75.8 ± 6.5 years) and nine age-matched ($p>0.10$) subjects with normal cognition (CN, Avg. age 69.0 ± 8.0 years). In our CD group, two subjects have previously been diagnosed with AD, two have been diagnosed with positive mild cognitive impairment, and two had no specific diagnosis. Averages of $|G^*|$ and OSS-SNR of each brain region listed above were performed and compared between CD, CN, and young adult groups using unpaired, 1-tailed, t-tests.

RESULTS

Using our phantom as validation of accuracy and as a rationale for using ultra-high resolution MRE to investigate small brain regions, the calculated shear stiffness values are within the manufacturer's specified range ($1.667 \pm 0.333\text{kPa}$) at both 2.5mm^3 ($1.425 \pm 0.006\text{kPa}$) and 1.1mm^3 resolutions ($1.423 \pm 0.010\text{kPa}$). However, at 2.5mm resolution, the inclusion (specification $2.667 \pm 0.333\text{kPa}$) is not in the correct range at a mean of only 1.765kPa , but is in the correct range at 1.1mm resolution at a mean of 2.393kPa (Figure 1).

Investigating the advanced post-processing techniques on the 20 young healthy human subjects, we observed a whole-brain average 127% significant increase in OSS-SNR using just denoising and a 375% significant increase using both advanced reconstruction and denoising. Using advanced reconstruction, we observed the removal of artifacts introduced by scanner reconstruction error (Figure 2a). Investigating differences between CN and CD groups in regional averages of $|G^*|$, we observe a significant decrease in $|G^*|$ in each brain region apart from the EC (12.6% decrease in WB*, 13.0% in GM*, 14.8% in WM*, 19.1% in FL*, 15.0% in PL*, 19.6%** in TL, and 17.9% in HC**; * $p<0.05$; ** $p<0.01$; Figure 2b). Additionally, we observe a significant decrease in $|G^*|$ between young adult and CN groups in WB (12.5%*), GM (11.6%*), WM (16.8%*), TL (11.4%**) and HC (20.6%**) simply due to the effect of aging (* $p<0.05$; ** $p<0.01$; Figure 2b).

DISCUSSION

Overall, this work successfully developed and implemented low noise, high resolution MRE at ultra-high field (7T) to determine the mechanical properties of small brain tissue structures, showing

regional differences in brain stiffness in subjects with cognitive deficits. Our initial phantom validation experiments clearly indicate the motivation for use of high resolution MRE in investigating small structures with accuracy, achieved using 7T. Additionally, we can achieve high OSS-SNR at this high resolution by using both denoising and post-hoc advanced reconstruction, as denoising removes thermal and gaussian noise while advanced reconstruction removes errors caused by the scanner reconstruction. Noise reduction in the case of scanner subjects with cognitive deficits is of particular importance, as it also allows us to keep the scan time relatively short by removing the noise cause by acceleration techniques.

Using these advanced techniques and high resolution allows us to observe differences in smaller brain structures than previous investigations, and with a higher level of accuracy. These previous investigations at courser resolutions (3mm^3 or 2.5mm^3)^{2,3,5,6} typically only investigate larger regional or WB differences between groups, or report particularly low values of smaller regions such as HC⁶ compared to what is reported in this study. A more recent study using a slightly higher resolution (1.6mm^3) reported changes in individual lobes of HC in subjects with AD⁴, which can likely be further observed with our ultra-high resolution. This more accurate information on smaller structures will allow us to better investigate neurodegeneration *in vivo*.

However, this study does have limitations that need to be addressed as analysis continues. First, a more robust inversion algorithm, such as nonlinear inversion¹⁹ would benefit the high-resolution scan, resulting in even more detail. Additionally, individual corrections for changes in brain volume, age, and sex would allow for more accurate comparison between groups²⁰. Finally, this study has a relatively small sample size of individuals with CD, although recruitment is still ongoing.

ACKNOWLEDGEMENTS

We acknowledge support from NSF CMMI 1953323 and NIH funding R21AG071179.

REFERENCES

- [1] Muthupillai, *et al.*, *Magn Reson Med*, 1996
- [2] Murphy, *et al.*, *NeuroImage Clin*, 2016
- [3] Murphy, *et al.*, *J. Magn. Res. Img.*, 2011
- [4] Hiscox, *et al.*, *Brain Commun*, 2019
- [5] ElSheikh, *et al.*, *AJR Am J Roentgenol*, 2017
- [6] Gerischer, *et al.*, *Clin. Neurophys.*, 2016
- [7] Marshall, *et al.*, *First MRE Workshop Berlin*, 2017
- [8] Barnhill, *et al.*, *Proc. ISMRM 2016*
- [9] McGarry, *et al.*, *Phys Med Biol*, 2011
- [10] Murphy, *et al.*, *PLoS One*, 2013
- [11] Triolo, *et al.*, *Proc. SB3C 2021*
- [12] Triolo, *et al.*, *Proc. ISMRM 2021*
- [13] Triolo, *et al.*, *Curr Protoc*, 2022
- [14] Veraart, *et al.*, *NeuroImage*, 2016
- [15] Hansen & Sørensen, *Magn Reson Med*, 2013
- [16] Karsa & Shmueli, *IEEE Trans Med Imaging*, 2019
- [17] Reuter, *et al.*, *NeuroImage*, 2019
- [18] SPM12
- [19] McGarry, *et al.*, *Med Phys*, 2012
- [20] Sack, *et al.*, *PLoS One*, 2011